ELSEVIER
www.elsevier.com/locate/ophopt

Ophthal. Physiol. Opt. Vol. 21, No. 5, pp. 384–392 2001

0275-5408/01/$20.00

PII: S0275-5408(01)00006-0

Spatially resolved polarization properties for *in vitro* corneas

Juan M. Bueno[1] and Jaroslaw Jaronski[2]

[1]Laboratorio de Óptica, Universidad de Murcia, Campus de Espinardo (Edificio C), 30071, Murcia, Spain and [2]Physiological Optics Group, Institute of Physics, Wroclaw University of Technology, Wybrzeze Wyspianskiego 27, 50-370 Wroclaw, Poland

Summary

Spatially resolved polarization properties of *in vitro* mammalian corneas have been studied by using a Mueller-matrix imaging polarimeter in transmission mode. Sixteen images corresponding to independent combinations of polarization states in the illumination and analyzing pathways are recorded. Spatially resolved Mueller matrices of the samples are calculated from them. Results show that the birefringence of the cornea is almost linear. Although the magnitude of retardation depends on the sample, it is approximately constant at the center and increases towards the periphery. Dichroism and polarizing power are negligible. Maps of the degree of polarization indicate that the cornea basically does not depolarize the totally polarized incident light. © 2001 The College of Optometrists. Published by Elsevier Science Ltd. All rights reserved.

Introduction

Methods using polarized light could be very useful in investigations of the lamellar structure of the cornea. The polarized light passing through the cornea changes its polarization state giving information about its optical and mechanical properties. Although the cornea is usually divided into several layers, its birefringence is due to the stroma, which makes up nine-tenths of the corneal thickness (Bour, 1991). The stroma is composed of layers of collagenous fibers, called lamellae. Fibers within each individual lamella are parallel, but make large angles with adjacent lamellae. From the physical point of view, there are two different sources of corneal birefringence (Born and Wolf, 1980): (1) the intrinsic birefringence due to each individual fiber and (2) the form birefringence that has its origin in the stack formed by the lamellae.

Received: 19 June 2000
Revised form: 17 December 2000
Accepted: 14 February 2001

Correspondence and reprint requests to: Juan M. Bueno, School of Optometry, University of Waterloo, Waterloo, Ontario, Canada N2L 3G1. Tel.: +1-519-888-4567, ext. 6210; fax: +1-519-725-0784.
E-mail address: bueno@um.es (J. M. Bueno).

Although the physical nature of corneal birefringence was recognized early (see Bour (1991) for a general review), different and sometimes contradictory models of the corneal anisotropy are present in the literature. Furthermore, many experimental works (in humans and animals) have reported different results of corneal birefringence measurements. Stanworth and Naylor first proposed a model of corneal anisotropy in which the lamellae are randomly oriented and the cornea behaves like a uniaxial crystal plate with its optical axis perpendicular to its surface (Naylor, 1953; Stanworth and Naylor, 1950). Moreover they found that for light incident normal to the corneal surface (isolated cat corneas), the retardation is basically zero, although it increases with the angle of incidence. Results by using a subjective technique (Bour and Lopes Cardozo, 1981) reported that for *in vivo* human corneas the ocular retardation increases from zero in the center of the pupil to a maximum at the margins. On the other hand, by using a scattered-light method, Post and Gurland (1966) studied the birefringence of the cornea of an enucleated cat eye, concluding that there are local regions where fibers are essentially parallel. Kaplan and Bettelheim (1972) found similar results for *in vitro* bovine corneas. Cope *et al.* (1978) and Shute (1974) also proposed a preferential orientation of human lamellae. McCally and Farell

(1982) suggested that in rabbit and bovine corneas the directions of the corneal lamellae are not random. There is either one preferred direction or two preferred directions that are orthogonal, although some lamellae are evidently oriented in all directions. Van Blokland and Verhelst (1987) measured the birefringence of *in vivo* human corneas using Mueller-matrix ellipsometry, showing that the cornea can be treated as a biaxial crystal and proposed the existence of a second slow axis due to a preferential direction of the stromal lamellae. They found that the retardation at the central area of the pupil plane is approximately constant (but greater than zero) and increases with eccentricity. Theoretical simulations of Donohue *et al*. (1995) confirmed that the lamellae orientations are not entirely random, but rather a significant fraction are oriented in a fixed, preferred direction. Jaronski and Kasprzak (1999) have recently measured the birefringence of *in vitro* human corneas by use of phase-stepping imaging polarimetry and have found that the distribution of retardation is nearly constant in the center of cornea but highly non-homogenous over the periphery.

Most of these previous studies were only centered on corneal birefringence and polarimetric techniques were not always used. However some authors have shown the usefulness of the Mueller-matrix polarimetry to assess the polarization properties of the eye (Bueno, 2000a; Bueno and Artal, 1999; Pelz *et al*., 1996; van Blokland, 1985).

The Mueller matrix (Chipman, 1995) of a system is a 4×4 matrix M with real valued elements M_{ij} (i, $j = 0$, 1, 2, 3) that contains information about all its polarization properties. On the other hand, the polarization state of a light beam is described by a four-element column vector known as Stokes vector, which can be located on the so-called Poincaré sphere (Jerrard, 1954). A change in the polarization state of an incident beam produced by a system is a linear transformation in a four-dimensional space. Nevertheless, the parameters characterizing the polarizing properties of the system do not appear explicitly in its Mueller matrix. In order to obtain useful information, theorems of polar decomposition are required (Gil and Bernabeu, 1987; Lu and Chipman, 1996). In general, the M_{00} element represents the intensity profile of the emergent beam when non-polarized light is entering the system. Elements M_{01}, M_{02} and M_{03} describe the diattenuation or dichroism (D) (attenuation between two orthogonal polarization states). M_{10}, M_{20} and M_{30} characterize the polarizance (P) (possibility of increasing the degree of polarization of a non-polarized incident light). All elements contribute to the calculation of the degree of polarization (DOP) of the system and, in addition, the lower 3×3 sub-matrix contains information on the retardation introduced by its birefringent structures. DOP, P and D range from 0 to 1 and

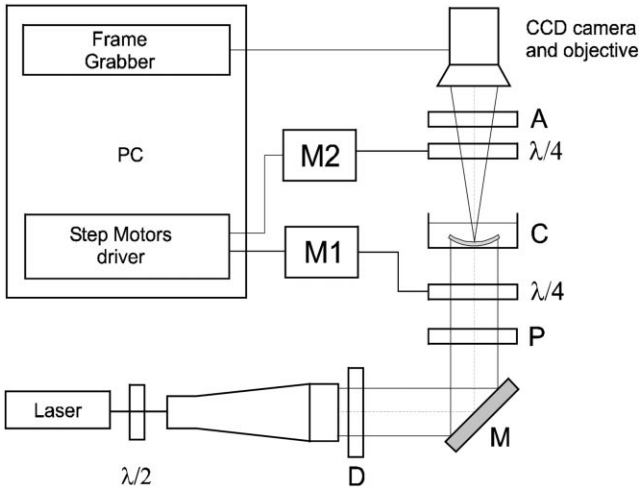

Figure 1. Schematic diagram of the Mueller-matrix imaging polarimeter used for *in vitro* measurements of corneal polarization properties. λ/2, half-wave plate; D, diffuser; P and A, horizontal linear polarizers; λ/4, quarter-wave plates; C, sample (*in vitro* cornea); M, mirror; M1 and M2, step motors.

are defined respectively as (Chipman, 1995):

$$D = \frac{\sqrt{M_{01}^2 + M_{02}^2 + M_{03}^2}}{M_{00}} \qquad P = \frac{\sqrt{M_{10}^2 + M_{20}^2 + M_{30}^2}}{M_{00}}$$

$$DOP = \frac{\sqrt{(\sum_{i,j=0}^{3} M_{ij}^2) - M_{00}^2}}{\sqrt{3} \cdot M_{00}} \tag{1}$$

The aim of the present work is to study more completely the spatially resolved polarization properties of the cornea, apart from its birefringence. It is centered on the analysis of the spatially resolved polarization properties of some non-human *in vitro* corneas. These properties are calculated from spatially resolved Mueller matrices (Bueno and Artal, 1999; Pezzaniti and Chipman, 1995) measured by using an imaging polarimeter.

Methods

Experimental setup: Mueller-matrix imaging polarimeter

Figure 1 shows a schematic diagram of the apparatus we have used to calculate spatially resolved Mueller matrices. The light source is a 633 nm He–Ne laser. The laser beam passes through a half-wave plate (λ/2) (used to rotate the linearly polarized laser beam to a horizontal position), is expanded, collimated, and reaches the Polarization-State Generator (PSG) composed of a fixed (horizontal) linear polarizer (P) and a rotating retarder (λ/4). After passing through the sample under study (C), the light enters the Polarization-State Analyzer (PSA) with a symmetrical

arrangement as the PSG ($\lambda/4$ and analyzer, A). A photographic objective conjugates the plane of the cornea with the CCD plane. The step motors (M1 and M2, used to rotate the retarders) and the CCD camera are controlled by a PC. A rotating diffuser (D) breaks the laser coherence to avoid the speckle in images. A series of 16 images of six *in vitro* corneas of two different animal species (three bovine and three porcine) (40 ms exposure time and 256×256 pixels with 8 bits/pixel) corresponding to independent combinations of polarization states PSG–PSA were recorded. Each pixel in the image corresponds to 0.04 mm in the plane of the sample.

Whole eyes were obtained from a local slaughterhouse and moved to the laboratory in containers with ice. Eyes were dissected, corneas extracted and placed in a transparent chamber filled with physiological saline solution. They were analyzed approximately 5 h after enucleation. Corneas were allowed to maintain their own shape during the experiment. There are two main reasons for such an arrangement: (1) to preserve corneal properties during the experiment and (2) minimize the refractive power of the cornea. Only subjective criteria were used to assess corneal clarity. However, none of the corneas used in the present study showed opacities or lack of transparency before being analyzed.

Prior to recording images of the samples under study, the complete setup was calibrated to determine the precision and accuracy of the instrument. A commercially available and non-depolarizing well-defined wedge made of crystalline quartz was used. Retardation and azimuthal angle were calculated and compared to the expected values. Systematic errors, estimated at 1–3%, were similar to other results in the literature (Bernabeu and Gil, 1985; Bueno, 2000b; Bueno and Artal, 1999; Fendrich *et al.*, 1994).

Theory: determination of spatially resolved Mueller matrices

Both the PSG and PSA consist of a fixed horizontal linear polarizer and a rotating quarter-wave plate. The Stokes vector of the light going into the first retarder is $(I_p, I_p, 0, 0)^T$ with I_p the intensity of the beam. The polarization states generated by the PSG are represented by the Stokes vector S_{PSG}:

$$S_{PSG} = \begin{pmatrix} S_0 \\ S_1 \\ S_2 \\ S_3 \end{pmatrix} = I_p \cdot t_1 \begin{pmatrix} 1 \\ c^2 \\ s \cdot c \\ s \end{pmatrix} \tag{2}$$

where $c = \cos 2\alpha$, $s = \sin 2\alpha$, and α and t_1 are the azimuth of the fast axis and the transmittance of the retardation plate, respectively.

The Mueller matrix of the system M, transforms the incident Stokes vector S_{PSG} into the output Stokes vector S'. For the PSA, the resulting Mueller matrix is:

$$\overline{M}_{PSA} = M^0_{pol} \cdot M^{\alpha'}_{\lambda/4} = \frac{t_2}{2} \begin{pmatrix} 1 & c'^2 & s' \cdot c' & -s' \\ 1 & c'^2 & s' \cdot c' & -s' \\ 0 & 0 & 0 & 0 \\ 0 & 0 & 0 & 0 \end{pmatrix} \tag{3}$$

where $c' = \cos 2\alpha'$, $s' = \sin 2\alpha'$, and α' and t_2 are the azimuth and transmittance of the second retarder respectively. In summary, every Stokes vector S_{PSG} passing through the entire setup and reaching the recording stage becomes $S_D = \overline{M}_{PSA} \cdot M \cdot S_{PSG}$. The first element of S_D is the intensity of the image (Shurcliff, 1962) recorded by the camera and given by:

$$I_D = \frac{I_p}{2} t_1 \cdot t_2 \cdot \left[\sum_{i=0}^{3} M_{0i} \cdot S_i + c'^2 \sum_{i=0}^{3} M_{1i} \cdot S_i + s' \cdot c' \sum_{i=0}^{3} M_{2i} \cdot S_i - s' \sum_{i=0}^{3} M_{3i} \cdot S_i \right] \tag{4}$$

This expression includes the 16 elements of the Mueller matrix of the sample. To calculate those elements four independent polarization states in both PSG and PSA are required (Hauge, 1978). When using a fixed linear polarizer and a rotating retarder, the four independent polarization states depend on the azimuth of the plate. In this case, azimuths of -45, 0, 30 and 60° ($\alpha_i = \alpha_i'$; ($i = 1, 2, 3, 4$) were chosen (Ambirajan and Look, 1995).

Let M_{PSG} and M_{PSA} be the auxiliary 4×4 matrices for both the PSG and the PSA:

$$M_{PSG} = I_p \cdot t_1 \begin{pmatrix} 1 & 1 & 1 & 1 \\ c_1^2 & c_2^2 & c_3^2 & c_4^2 \\ s_1 \cdot c_1 & s_2 \cdot c_2 & s_3 \cdot c_3 & s_4 \cdot c_4 \\ s_1 & s_2 & s_3 & s_4 \end{pmatrix}$$

$$M_{PSA} = t_2 \begin{pmatrix} 1 & c_1^2 & s_1 \cdot c_1 & -s_1 \\ 1 & c_2^2 & s_2 \cdot c_2 & -s_2 \\ 1 & c_3^2 & s_3 \cdot c_3 & -s_3 \\ 1 & c_4^2 & s_4 \cdot c_4 & -s_4 \end{pmatrix} \tag{5}$$

where M_{PSG} is the matrix whose columns are the four independent Stokes vectors S_{PSG} (Eq. (2)) and M_{PSA} is the matrix with each row being the first row of every $\overline{M}_{PSA}$ (Eq. (3)).

For each independent PSG–PSA combination one image $I_D^{(i\_j)}$ ($i, j = 1, 2, 3, 4$) is recorded. The relationship between every spatially resolved Stokes vector $S'^{(i)}$ going out of the

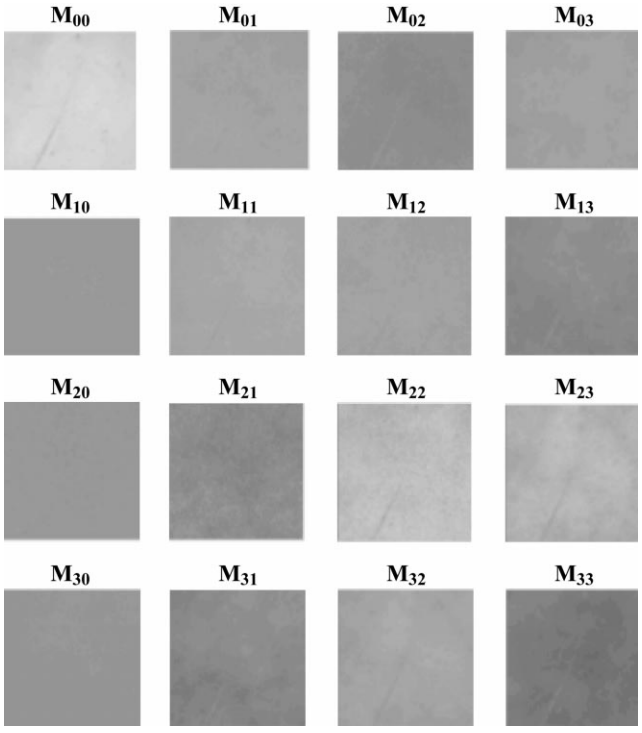

Figure 2. Images corresponding to the elements of the spatially resolved Mueller matrix for an isolated cornea (bovine, 10×10 mm). Each image represents an element of the matrix. Gray level ranges from -1 (black) to 1 (white).

sample and the recorded images is given by:

$$I_{\mathrm{D}}(i) = \begin{pmatrix} I_{\mathrm{D}}^{(i\_1)} \\ I_{\mathrm{D}}^{(i\_2)} \\ I_{\mathrm{D}}^{(i\_3)} \\ I_{\mathrm{D}}^{(i\_4)} \end{pmatrix} = \frac{1}{2} \cdot M_{\mathrm{PSA}} \cdot S'^{(i)} \tag{6}$$

where $I_{\mathrm{D}}^{(i)}$ $(i = 1, 2, 3, 4)$ is an auxiliary vector containing the images corresponding to a fixed PSG state and four PSA states. If $M_{\mathrm{S\_OUT}}$ is the auxiliary 4×4 matrix with its columns being the four vectors $S'^{(i)}$ (calculated by means of the inversion of Eq. (6)), the experimental spatially resolved Mueller matrix of the sample is finally obtained from:

$$M = M_{\mathrm{S\_OUT}} \cdot (M_{\mathrm{PSG}})^{-1} \tag{7}$$

Results

By using the procedure shown in the previous section, a Mueller matrix is obtained at each pixel of the image. Spatially resolved Mueller matrices were measured for several in vitro corneas. As an example, *Figure 2* shows the gray scale images representing the 16 components of the Mueller matrix for a bovine cornea. Each image represents a central area of the cornea (10×10 mm). From the Mueller matrices and by using the polar decomposition theorem reported by Lu and Chipman (1996) the spatially resolved parameters of polarization have been calculated.

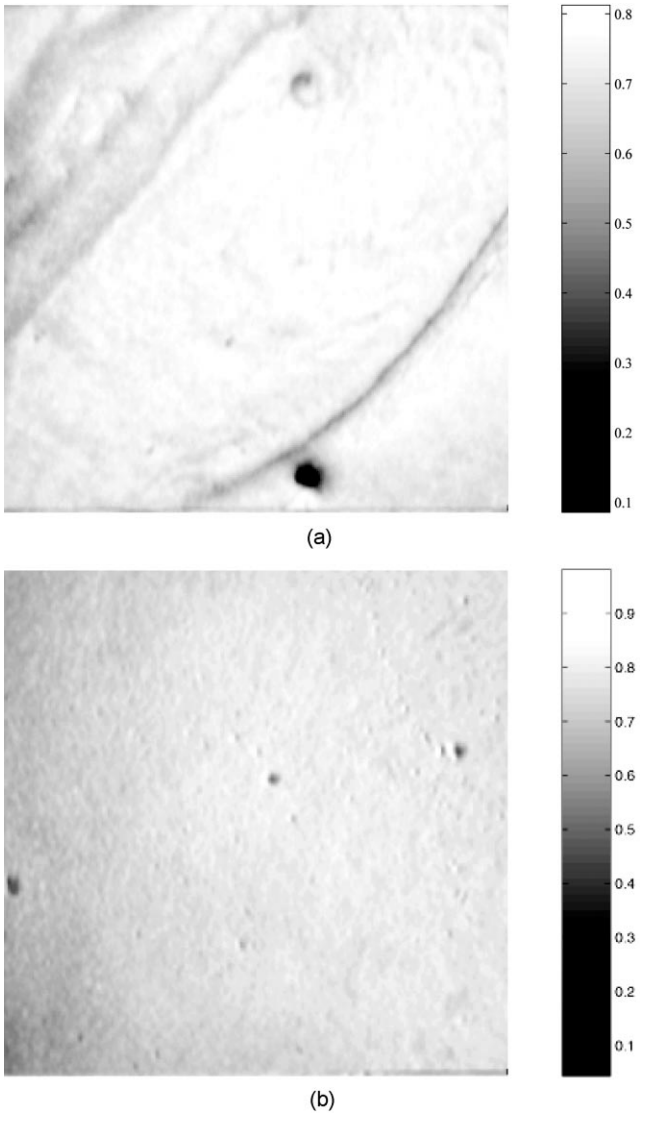

Figure 3. Spatially resolved degree of polarization for two different *in vitro* corneas: (a) porcine, (b) bovine. Each image has a full size of 10 mm.

Figure 3 presents maps for the DOP corresponding to two corneas. Spots and irregularities in distributions are attributed to noisy pixels and small wrinkles in the samples. The average values for these images were 0.80 ± 0.01 and 0.92 ± 0.02.

The spatially resolved diattenuation of two different samples (calculated by using Eq. (1)) are shown in *Figure 4*. This parameter is close to zero (minimum value for D), which means that the properties of dichroism of the cornea are negligible.

The polarizing power of a system is specified by the first column of its Mueller matrix (see Introduction), and

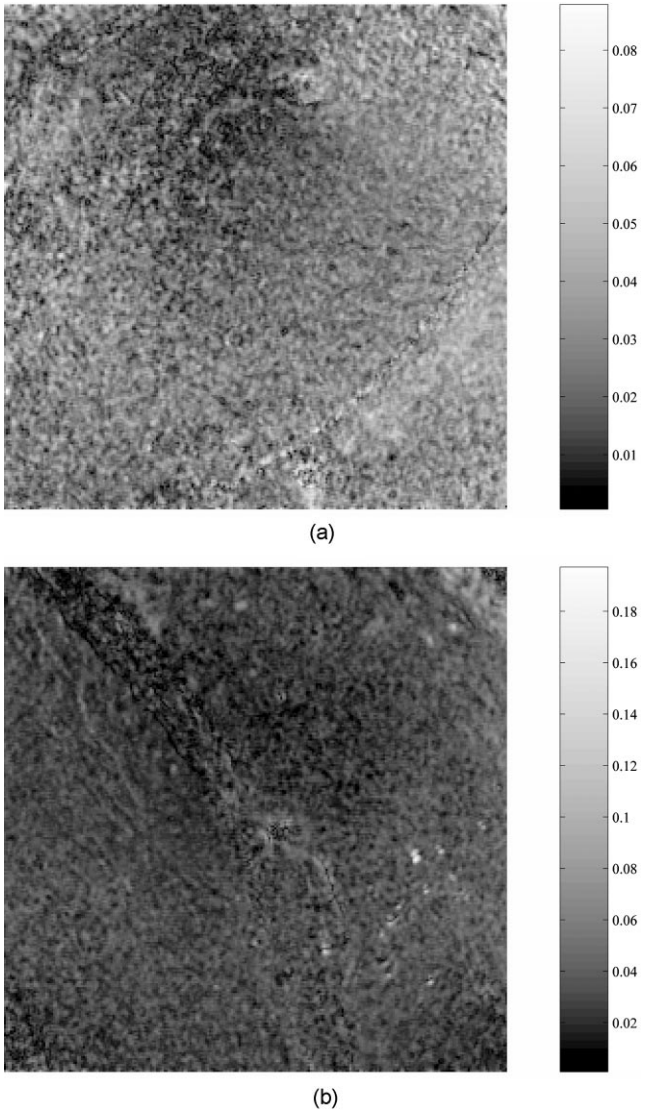

Figure 4. Maps of corneal diattenuation for two corneas: (a) porcine, (b) bovine. Images subtend the same as in previous figure.

elements M_{10}, M_{20} and M_{30} correspond to the spatially resolved polarizance vector (Lu and Chipman, 1996). Taking *Figure 2* into account, those elements are near zero (0.007 ± 0.004, -0.006 ± 0.005 and -0.008 ± 0.004 on average for M_{10}, M_{20} and M_{30}, respectively), which indicates that the cornea itself cannot increase the degree of polarization of the non-polarized incident light. The distribution of polarizance (Eq. (1)) for one of the samples is given in *Figure 5*.

Spatially resolved ellipticity for two corneas is shown in *Figure 6*. This parameter refers to the ellipticity of the equivalent retarder associated with the birefringent structure of the system under study (Gil and Bernabeu, 1987; Lu and Chipman, 1996). The parameter seems to be close to zero (which implies linear birefringence) and uniform (gray

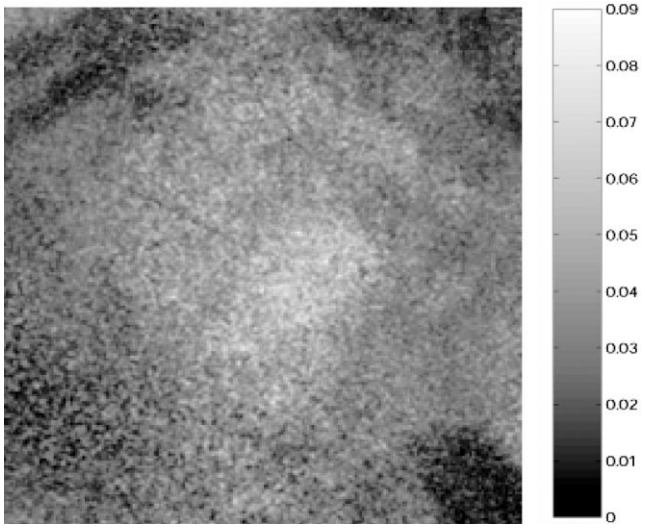

Figure 5. Distribution of polarizance for an *in vitro* cornea (porcine, 10×10 mm). Average across the image 0.059, standard deviation 0.035.

scales are normalized between the maximum and the minimum for each image).

Figure 7 shows the retardation introduced at each point by a porcine cornea (mean $99.2 \pm 3.7°$). Averages for all the samples and the whole images were 98.2 ± 1.1 and $95.5 \pm 0.7°$ for porcine and bovine corneas, respectively. This parameter reflects the fluctuations of corneal thickness and local disturbances in corneal structure. For a better discrimination, averaged values of retardation (for all the samples) along a horizontal meridian across the middle of the image are presented in *Figure 8*. Results for a vertical meridian were similar. Retardations associated with corneal birefringence are approximately constant at the central part although they increase slightly towards the periphery.

Finally, *Figure 9* presents the distribution of azimuthal angle. Averages for the images are -23.0 ± 1.9 and $0.3 \pm 0.5°$, indicating that this parameter does not have a clear tendency and depends on each sample.

Discussion and conclusions

An imaging polarimeter in transmission mode using rotating retarders has been used to measure spatially resolved Mueller matrices of *in vitro* corneas. These Mueller matrices are obtained by means of a matrix-inversion method and a Fourier analysis of the signal is not required (Bernabeu and Gil, 1985; Pezzaniti and Chipman, 1995; van Blokland, 1985).

Results of spatially resolved polarimetry show the following. The average DOP for all samples (whole images) was 0.90 ± 0.10. Since the DOP during the calibration of the system was estimated at 0.93, corneas of porcines and bovines do not present large effects of depolarization. Although some maps of DOP have non-significant noisy

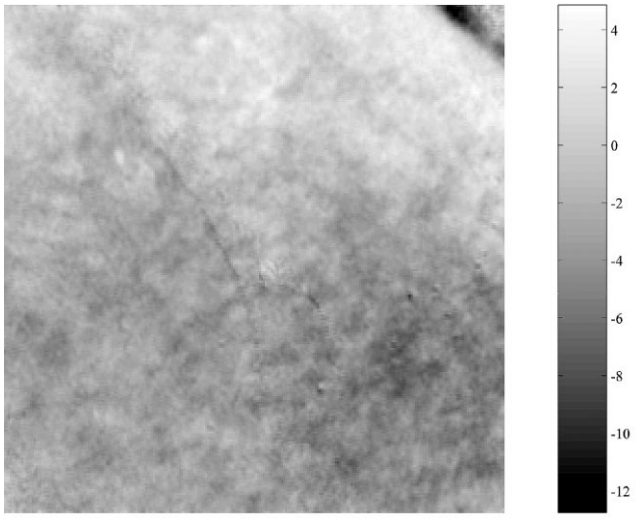

(a)

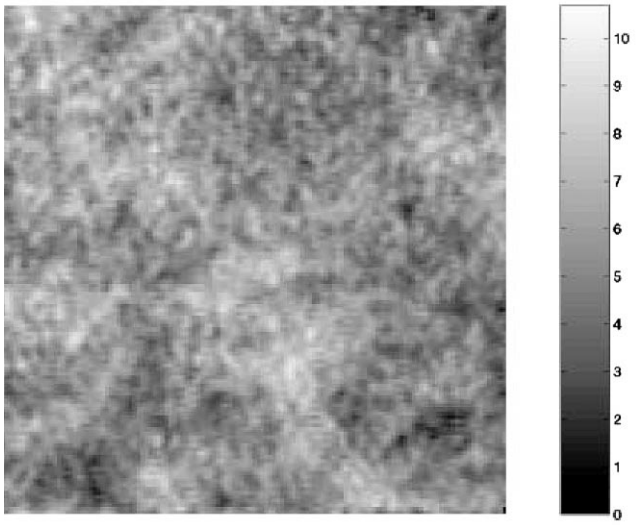

(b)

Figure 6. Spatially resolved ellipticity for two *in vitro* corneas: (a) porcine, (b) bovine. The size of each image is the same as in previous figures. Units are °.

areas (probably resulting from handling of the samples before the analysis), in general, they are uniform. This uniformity indicates that the corneal structure is quite regular and sources of scattering or diffusion that could reduce the DOP are not so important.

Although many previous experiments studied the depolarization of the light in the ocular media, contradictory results have been reported. While some authors found a complete depolarization of the light reflected at the retina (Brindley and Willmer, 1952; Vos *et al.*, 1965), others showed a substantially preservation (0.85 on average) (Bueno and Artal, 1999; Charman, 1980; van Blokland, 1985; Weale, 1966). However, all the studies reporting a decrease in the DOP located the depolarization effect at

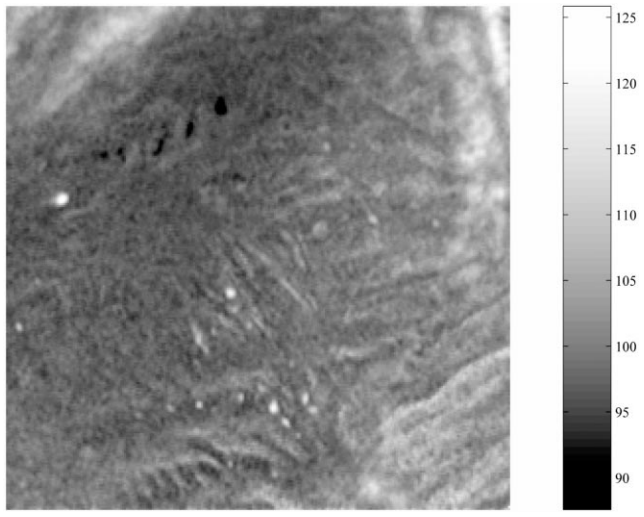

Figure 7. Map of retardation (in °) for an *in vitro* porcine cornea.

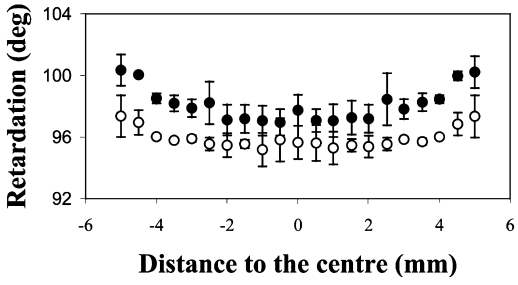

Figure 8. Horizontal averaged profiles of retardation for the two groups of corneas (black circles, porcine; white circle, bovine). Error bars indicate the standard deviation. 0-mm position corresponds to the center of the image.

the fundus. Pelz (1997) calculated the contribution of the central cornea to the polarization properties of the *in vivo* human eye using the light coming back from the first surface of the lens, finding that the depolarization due to the cornea is not significant. Our results for non-human corneas agree with those found by Pelz (1997).

The average diattenuation (whole images and all samples) was 0.03 ± 0.01. This indicates that the transmittance of the cornea does not depend on the incident polarization state and dichroic properties are negligible (only a birefringent structure will be present). This implies that the main change in the polarization state of the light passing through the cornea will be basically represented on the Poincaré sphere by a rotation around an eigenvector. Previous studies (Bour, 1991) proposed the retina as the only source for dichroism. However, to our knowledge data referring to corneal diattenuation itself have not been previously reported.

The spatially resolved corneal polarizing power is shown in *Figure 2* (elements M_{10}, M_{20} and M_{30}) and *Figure 5*. The

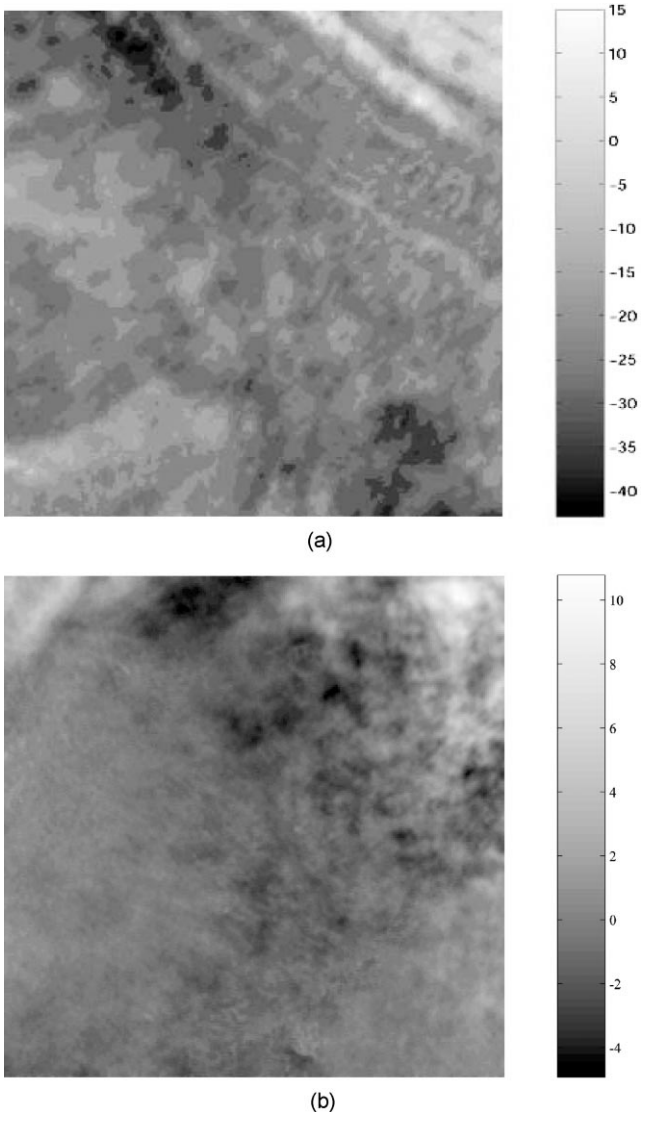

Figure 9. Data of corneal azimuth (orientation of the eigenvector) in ° for the enucleated cornea of a porcine (a) and a bovine (b). Zero is horizontal and angles increase anti-clockwise when looking into the eye.

averaged polarizance for these corneas was 0.05 ± 0.01, what indicates that if non-polarized light passes the cornea, it will not basically increase its DOP. A polarizing effect of the human eye was previously reported but it was attributed to the retina (Röhler *et al*., 1969).

Data of ellipticity (*Figure 6*) show that the location of the eigenvector of the birefringent structure is close to the equator (the average was $0.25 \pm 2.32°$). This means that the corneal birefringence is linear, that is, the presence of optical activity (or circular birefringence) does not contribute much to modify the state of polarization. Most previous studies (in both humans and animal) reported this linear birefringence for the cornea (Bour, 1991) and for the whole eye (Bueno, 2000a; van Blokland, 1985). However, recent experiments have suggested the presence of circular birefringence (Pierscionek and Weale, 1998). Our results, based on the calculation of the Mueller matrices do not show this contribution. Some media exhibit circular birefringence along the optical axis but they are linearly birefringent in other directions (Jenkins and White, 1976). There is, therefore, a continuous change from circular to linear birefringence, depending on the angle of incidence. Probably the circular birefringence reported by Pierscionek and Weale (1998) is a result of using wide angles (with respect to the line of gaze) for illumination and recording pathways instead of perpendicular incidence (similar to ours).

Figure 8 shows that the corneal retardation for different animals has a common behavior. Results presented here confirm that the minimum retardation is observable at the central part of the cornea. At that area, the parameter is approximately constant (which indicates a constant thickness and a homogeneous corneal structure there), but it increases slightly when going towards the periphery. In addition, our data show that the retardation follows a simple curve that looks like a fourth-order function ($R = 0.95$, $p < 0.0001$ and $R = 0.96$, $p < 0.0001$, for porcine and bovine corneas, respectively) which indicates a smooth variation in retardation.

Kaplan and Bettelheim (1972) measured the optical retardation of bovine corneas and found an increase in retardation from 80° at the center to 200° at 1 cm, for light of 633 nm. However, they supposed that the corneal thickness was uniform, which is extremely unlikely. Our results at the center of the cornea are similar.

Other early experiments found ocular fixed retardations ranging from 30 to 90° (Boehm, 1940; Cope *et al*., 1978; de Vries *et al*., 1953; Shute, 1974). Stanworth and Naylor (Naylor, 1953; Stanworth and Naylor, 1950) and Bour and Lopes Cardozo (1981) measured the corneal retardation across the pupil plane reporting that it increased from zero in the center to about 50–100° at the margin. Van Blokland and Verhelst reported that although there is a large variability among subjects, the corneal retardation is non-null and approximately constant at the central area of the pupil plane (55° on average) and increases with eccentricity (for some subjects larger that 200°). Jaronski and Kasprzak (1999) also found an increase in retardation by but they did not report numerical values. Our results show only a slight increase along the radius. Since there is a direct relationship between the retardation and the thickness of a birefringent sample, retardations at the central cornea could be larger than those found for human eyes due to differences in corneal thickness among different mammalians.

On the other hand, the distribution of azimuth (*Figure 9*) is probably related to the orientation of the corneal lamellae. Azimuths for *in vitro* samples were reported to be uniform at the central part of the cornea (Kaplan and Bettelheim, 1972). Most previous experiments (Bour, 1991; Pelz,

1997) reported that the corneal slow axis was along a nasal-downward direction (between 0 and 40°), although a non-uniform distribution has been recently shown (Jaronski and Kasprzak, 1999). Because we did not know if corneas corresponded to right or left eyes and we did not take into account the orientation of the cornea in the experimental set up, comparisons can not be done for this parameter.

The spatially resolved study of the cornea allows an examination of its structure and lamellar arrangement. Investigation of the corneal birefringence could be useful in medical diagnosis of corneal pathologies (i.e. keratoconus) and have some potential applications in transplantation of human corneas and refractive surgery procedures.

To summarize, maps of different parameters of polarization of *in vitro* corneas have been calculated by using spatially resolved Mueller matrices. With these distributions a more complete description of the spatial changes in the state of polarization of the light passing through the cornea is obtained. Results show that the corneal birefringence is linear (ellipticity almost null) and the retardation approaches circularly symmetrical behavior increasing from center to periphery. Properties of dichroism are negligible and effects of depolarization are not so significant. When non-polarized light is incident, the cornea does not have a polarizing effect. Although the eye has rather complicated polarization properties, the results obtained from our study indicate that the cornea contributes mostly with its birefringent structure. Because the lens is only slightly birefringent (klein Brink, 1991) the remaining polarization properties could be attributed to the retina.

Acknowledgements

The authors thank Jennifer Hunter for suggestions on, and revisions to the manuscript.

References

Ambirajan, A. and Look, D. C. (1995). Optimum angles for a polarimeter: part I. *Opt. Eng.* **34,** 1651–1655.

Bernabeu, E. and Gil, J. J. (1985). An experimental device for the dynamic determination of Mueller matrices. *J. Optics (Paris)* **16,** 139–141.

Boehm, G. (1940). Ueber maculare (Haidingersche) Polarisations buschel und ueber einen polarisationoptischen Fehler des Auges. *Acta Ophthalmol.* **18,** 109–169.

Born, M. and Wolf, E. (1980). *Principles of Optics*. 6th ed, Pergamon Press, New York.

Bour, L. J. (1991). Polarized light and the eye. (ed W. N. Charman), In: *Vision Optics and Instrumentation*, 1, CRC Press Inc, Boston, MA, USA, p. 13.

Bour, L. J. and Lopes Cardozo, N. J. (1981). On the birefringence of the living human eye. *Vision Res.* **21,** 1413–1421.

Brindley, G. S. and Willmer, E. N. (1952). The reflexion of light from the macular and peripheral fundus oculi in man. *J. Physiol.* **116,** 350–356.

Bueno, J. M. (2000a). Measurement of parameters of polarization in the living human eye using imaging polarimetry. *Vision Res.* **40,** 3791–3799.

Bueno, J. M. (2000b). Polarimetry using liquid-crystal variable retarders: theory and calibration. *J. Opt. A: Pure Appl. Opt.* **2,** 216–222.

Bueno, J. M. and Artal, P. (1999). Double-pass imaging polarimetry in the human eye. *Opt. Lett.* **24,** 64–66.

Charman, W. N. (1980). Reflection of plane-polarized light by the retina. *Br. J. Physiol. Opt.* **34,** 34–49.

Chipman, R. A. (1995). Polarimetry. In: *Handbook of Optics*, 2nd ed, McGraw-Hill, New York, USA, p. 22.

Cope, W. T., Wolbarsht, M. L. and Yamanashi, B. S. (1978). The corneal polarization cross. *J. Opt. Soc. Am.* **68,** 1139–1141.

de Vries, H. L., Spoor, A. and Jielof, R. (1953). Properties of the eye with respect to polarized light. *Physica* **19,** 419–432.

Donohue, D. J., Stoyanov, B. J., McCally, R. L. and Farrell, R. A. (1995). Numerical modeling of the cornea's lamellar structure and birefringence properties. *J. Opt. Soc. Am. A* **12,** 1425–1438.

Fendrich, T., Fischer, S. K. and Bille, J. F. (1994). Development of an electro-optical ellipsometer with application in ophthalmology. *Proc. SPIE* **2079,** 76–82.

Gil, J. J. and Bernabeu, E. (1987). Obtainment of the polarizing and retardation parameters of a non-depolarizing optical system from the polar decomposition of its Mueller matrix. *Optik* **76,** 67–71.

Hauge, P. S. (1978). Mueller matrix ellipsometry with imperfect compensators. *J. Opt. Soc. Am.* **68,** 1519–1528.

Jaronski, J. W. and Kasprzak, H. T. (1999). Generalized algorithm for photoelastic measurements based on phase-stepping imaging polarimetry. *Appl. Opt.* **38,** 7018–7025.

Jenkins, F. A. and White, H. E. (1976). *Fundamentals of Optics*. 4th ed, McGraw-Hill, New York.

Jerrard, H. G. (1954). Transmission of light through birefringent and optically active media: the Poincaré sphere. *J. Opt. Soc. Am.* **44,** 634–640.

Kaplan, D. and Bettelheim, F. A. (1972). On the birefringence of bovine cornea. *Exp. Eye Res.* **13,** 219–226.

klein Brink, H. B. (1991). Birefringence of the human crystalline lens *in vivo*. *J. Opt. Soc. Am. A* **8,** 1788–1793.

Lu, S. and Chipman, R. A. (1996). Interpretation of Mueller matrices based on polar decomposition. *J. Opt. Soc. Am. A* **13,** 1106–1113.

McCally, R. L. and Farrel, R. A. (1982). Structural implications of small-angle light scattering from cornea. *Exp. Eye Res.* **34,** 99–113.

Naylor, E. J. (1953). Polarized light studies of the corneal structure. *Br. J. Ophthal.* **37,** 77–84.

Pelz, B. C. E. (1997). *Entwicklung eines elektrooptischen Ellipsometers zur in vivo Evaluation der retinalen Nervenfaserschicht und der Hornhaut des menschlichen Auges*. Universität Heidelberg. PhD Thesis.

Pelz, B., Weschenmoser, C., Goelz, S., Fischer, J. P., Burk, R. O. W. and Bille, J. F. (1996). *In vivo* measurement of the retinal birefringence with regard on corneal effects using an electro-optical ellipsometer. *Proc. SPIE* **2930,** 92–101.

Pezzaniti, J. L. and Chipman, R. A. (1995). Mueller matrix imaging polarimetry. *Opt. Eng.* **34,** 1558–1568.

Pierscionek, B. K. and Weale, R. A. (1988). Investigation of the polarization optics of the living human cornea and lens with Purkinje images. *Appl. Opt.* **37,** 6845–6851.

Post, D. and Gurland, J. E. (1966). Birefringence of the cat cornea. *Exp. Eye Res.* **5,** 286–295.

Röhler, R., Miller, U. and Aberl, M. (1969). Zur Messung der Modulations-Ubertragungsfunktion des lebenden mensclichen Auges im reflektierten Licht. *Vision Res.* **9,** 407–427.

Shurcliff, W. A. (1962). *Polarized Light: Production and Use*, Harvard University Press, Cambridge, MA.
Shute, C. C. D. (1974). Haidinger's brushes and predominant orientation of collagen in corneal stroma. *Nature* **250,** 163–164.
Stanworth, A. and Naylor, E. J. (1950). The polarization optics of the isolated cornea. *Br. J. Ophthal.* **34,** 201–211.
van Blokland, G. J. (1985). Ellipsometry of the human retina *in vivo*: preservation of polarization. *J. Opt. Soc. Am. A* **2,** 72–75.
van Blokland, G. J. and Verhelst, S. C. (1987). Corneal polarization in the living human eye explained with a biaxial model. *J. Opt. Soc. Am. A* **4,** 82–90.
Vos, J. J., Munnik, A. A. and Boogaard, J. (1965). Absolute spectral reflectance of the fundus oculi. *J. Opt. Soc. Am. A* **55,** 573–574.
Weale, R. A. (1966). Polarized light and the human fundus oculi. *J. Physiol.* **186,** 925–930.